Silicate-perovskite (Si-Fe-Nb-Ca-Ti) lava flows in Tamilnadu

R. Ramasamy

Retired Project Adviser, Department of Civil Engineering, Indian Institute of Technology, Madras, Chennai

Abstract: *Field occurrences of Si-Fe-Nb-Ca-Ti rich low viscous lava flows are seen in some parts of Tamil Nadu. A notable thick flow (300x100x5m) is found on the northern bank of Hanuman River at Sambavarvadakarai* (09°00'N: 07°22'38"E) *near Thenkasi Town. The chemical composition of the lava is very similar to the composition of a silicate-perovskite. Though, the silicate-perovskite is a stable solid crystalline phase at lower mantle region of the Earth, such occurrences on the land surface are first time reported as lava flows. The quenched low viscous lava-flows are monomineralic rocks essentially composed of perovskite group of minerals including ferrosilite and other unidentified accessory silicate minerals. The bulk-*compositions *of lavas on the basis of 3 (O) atoms for perovskite structural formulae vary around* $Si_{0.394}$ $Fe_{0.298}$ $Nb_{0.215}$ $Ca_{0.155}Ti_{0.120}$ $Al_{0.061}K_{0.058}Y_{0.044}$ $Zr_{0.041}$ $Mg_{0.041}$ $Na_{0.039}$ $P_{0.018}$ *and* $Sr_{0.006}$. *PGE and REE are determined in association with Ag, Au, Pb and U in this lava. The notable transition elements such as Sc, Cu, Ni, Co, V, Cr and Mn are estimated as trace elements. Some F, Cl and S substitute for* O_2. *The entry of Nb, Zr, Si, Al, Y and REE) replace Ca and Ti from perovskite's crystal structure. A very high concentration of Fe over Mg indicates that, the lava was derived at lower mantle probably at core-mantle-boundary of the Earth (CMB). Sudden release of pressure by development of fissure at CMB, a plasma-plume might have been raised fast. Under ideal gas law state it is calculated that 1* m^3 *of material at this place completely transformed as a plasma plume which ascends through the fissure very rapidly maximum speed of 288 m/s without any loss of its potential energy under frictionless and cooling-free environment possible to emplace as rootless body / lava-flow on the Earth's surface.*

Keywords: *Silicate-perovskite lava flows, Post-perovskite, Nb-Perovskite, Bridgmanite, Core-Mantle Boundary (CMB).*

1. INTRODUCTION

Several types of silica undersaturated rocks such as carbonatite [1] nephelinite [2], kimberlite [3], komatite [4] phoschorite [5], magmatic sulphide [6] apatite-ilmenorutile [7] and iron oxide magmas [8] derived from mantle source were reported. Between 1996 and 2004 minor alkali-basaltic effusions often less than 1m^3 in volumes took place in several parts of Tamil Nadu [9]. Many carbonatite lava flows belong to these categories [10]. The lava flows of *Si-Fe-Nb-Ca-Ti* are of similar kinds. The chemical composition of lower mantle closely appears [11] to be perovskite (pv). The silica enrichment of the lava may indicate that it is more related to silicate-perovskite (spv), a stable solid crystalline phase at 2700 km below the Earth's surface. The very high iron enrichment indicates that spv has transformed into a stable solid phase [11, 12] of post-perovskite (ppv) near to core mantle boundary (CMB) at 2891 km depth. Such occurrences shed light on the composition interior of the Earth. It is mystery of the Earth that such low volume of effusions emplaceing on the land surface.

2. FIELD STUDIES

Tamil Nadu has been subjected to several tectonic deformations and reactivations since Precambrian Period and marked them as lineaments, circular or arc features (Fig-1). Magmatic rocks and volcanic rocks are emplaced along these fractures. The author considers that even hydrocarbon deposits occurring in the sedimentary formations are derived from lower mantle region [13]. Very low density atypical carbonatite lavas [10] are closely associated with Fe-Si-Nb-Ti lava flows. Such occurrence of 100x5x10 cm is found in Nalluranpatti located 5 km south-east of Palayam. Similar carbonatite lava with Fe-Nb-Ti oxide lava ocuur at 1.5 km NW of Mylampatti village near Palayam.. Basalt carrying vesicles filled calcite and zeolite occurs in a well section 200m north of Mylampatti. About 2 km east of Kadavur village Fe-Nb-Ca-Ti oxide occurs in a pegmatite which associates with anorthosite. A small road branching out to Karuppur village from the main road lying between Pudunattham (Puttanattam) and Kallupatti, two small Fe-Si-Nb-Ti flows occur at distances of 0.5 km (10x3x0.1m) and 1 km (20x5x0.20m) towards Karuppur village. Within the carbonatite complex of Tiruppattur two generations early formed apatite-ilmenorutile rock in carbonatite of Sevvattur and highly differentiated late formed apatite-

ISSN 2455-4863 (Online) www.ijisset.org *Volume: 2 Issue: 11 | November 2016*

ilmenorutile occur in ultramafics comprised with youngest ankerite-carbonatite occur in Onnakarai (14)

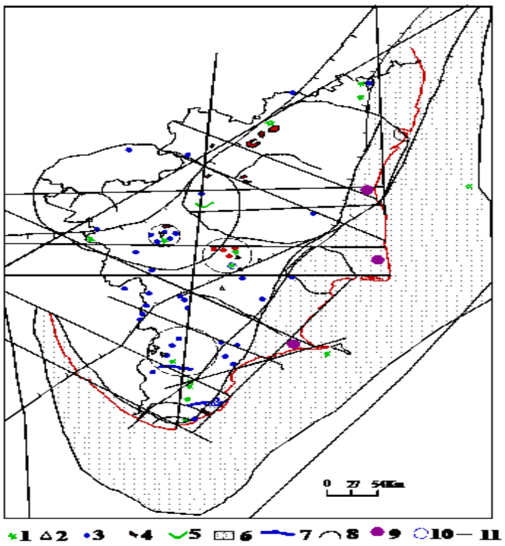

1 Basalt, 2 –Fe-Ca-Ti-Nb-Zr oxide effusives, 3-Carbonatite lavas

4 Alkali syenite carbonatite 5 Anorthosite 6 Sedimentary rocks

7 Kankar 8 Arc-shaped fractures 9 Petroleum Deposits 10 Circular

Features, 11 lineaments.

Fig 1: *Geological structure of Tamil Nadu*

Fig 2: *Columnar type of cooling is in Fe-Si-Nb-Ca-Ti lava. Similar features are found in SEM images (Fig-4)*

village. Fe-Si-Nb-Ti lava floats are strewn at 2 km north of Alanganallur at southern foot hill of Wagutamalai. A lava-flow of a size of 3x3x0.1 m occurs at northern foot hill of Udiyur village, 10 km south of Sivamalai alkaline complex. Here, carbonatite lava occurs in a circular fracture. Carbonatite lavas altered into kankar. Kankar occurring in arc-shaped structure is doubtful about its alteration from carbonatite-source. Relicts of unaltered low-density black coloured fine-grained pyroclastic-fragments of carbonatite-lava occur in Mio-Pliocene limestone of Kudangulam, Tisaiyanvilai, Sattangulam and Pannamparai villages. They are associated with kaolinization of host rocks of granitic gneisses all along

Fig 3: *Fe-Si-Nb-Ti lava beads and styles of pyroclastic fragments of lava in Sambavarvadakarai. The last two images show different views of a dead burnt man-made mud-pipe of 4 cm inner diameter encrusted by lava.*

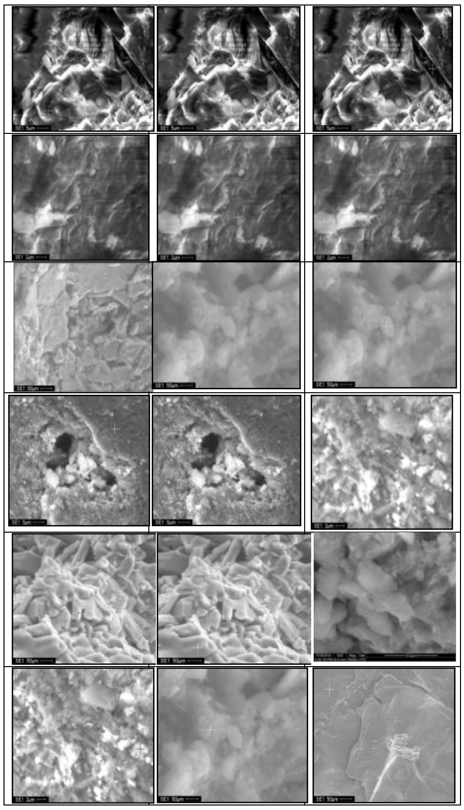

Fig 4: *SEM images of Perovskite lava flow at different parts of the sample*

southern coast of Tamil Nadu. About 10 km south-west of Vasudevanallur more than 3 occurrences of iron rich lava-flows occur in varying dimensions. Similarly about 6 km west of Kadayanallur 2 flows are cross-cutting a nallah. The Hanuman River lineament accompanies with several exposures of Fe-Si-Nb-Ti lava flows in NW and olivine-tephrite, soda-trachyte, carbonatite and carbonatite lava flows in SE of the lineament near Kudamgulam village [10]. Floats of such lava flows occur in Singikulam village, eastern foot hills of Vallanadu and other unknown places. Lava occurrence on the northern bank of Hanuman River in Sambavarvadakarai is the largest one of its kind. The average size of lava-flow is 300x100x5m (09°00'N: 07°22'38"E). The lava-flow was spread over a distance of 500 m towards northwest and tapering towards southeast 1 or 2 m. The thickness of the flow appears to be varied from a few cm to maximum of 7m emplaced over charnockitic gneiss. It appears to be a rootless body without any orifice. It is a very fine-grained rock and appears to be a molten iron alloy (Fig-2 and 3). It exhibits typical metallic lusture. Here and there a few vesicles are seen on the lava flow. Inner portions of the vesicles appear to be glossier. The bottom portion of lava flow is admixed with soil of clay, sand and grit. In some places columnar type of cooling features (Fig. 2 and Fig-4 in SEM images) are seen. Quenched materials are seen at bottom portions of the lava flows. Shape and size of vesicles vary from 100 x 50 x 20 mm^3 to a minimum < 0.1 mm diameter. The depth of vesicle varies widely and is equal or slightly more than that of its width. The cavities appear to be formed by escape of volatiles. Most cavities are planoconvex and very flat. It shows typical conchoidal fractures with sharp edges. It is so fine-grained; no minerals are identified either in naked eye or in thin sections under microscope. Flow structures such as layering, banding, necking, tailing, bulging, tapering, threading are clearly visible in naked eye. Several thin flow-bandings overlaps one over the other is seen. In the field, the sizes of flow bandings vary from >10 mm and thickness to >200 mm. The cross section of a large flow-band shows, chilled margins 2 to 3 mm thickness at both top and bottom portions. Inside some chilled walls, radiating sheaths and bundles of acicular crystals are seen with increasing length towards center. In central portion, cavities are similar to as in some pegmatite-vugs. The bulk densities of the lava samples vary from 4.26 to 7.92. This may be due to presence of cavities and pumice materials. Shape and size of other pyroclastic-fragments are shown in Fig.-3. They show that they are derived from low-viscous liquid. Beads are hollow inside. Their length and breadth ratio often exceeds over 3. Glassy threads and needles and tails of the lava materials are seen projecting as beads. Pele's hairs and threads are collected as evidence for rapid volcanic quenching. Funnel shaped body of a size 20cm length 10 cm diameter at the top and 2 cm at the bottom is collected. Most of the pyroclastic-fragments are more flattened. Some of them have tails at the end. Last two pictures in Fig-3 show man-made burnt mud-tube of 4 cm inner diameter. It is encrusted with lava flow indicating that the lava flow took place during early civilization of Tamil people (around 5000 years ago) lived in this village.

3. METHODOLOGY

Samples were collected during extensive field-work during several types of economic mineral investigations between 1974 and 2000 in the Tamil Nadu State Department of Geology and Mining. Wet gravimetric analyses of the samples were made. Nb, Zr, Y and other REE were not determined by wet gravimetric analyses. Using high resolution scanning electron microscope attached with electron energy diffusive x-ray micro-analytical probe (EDAX), SEM images and analyses were made in the Laboratory of Metallurgical Engineering and Material Science in the Indian Institute of Technology, Madras. The results were obtained according to elements input decided. If any critical element missed to input, may change the output of the result. Not estimation of Nb and Sr up to weight 20% in the samples present in Table-3 the output of weight % proportionately increased and correction measures are to be applied. Though such corrections were not made, the analyses show very high contents of Si and Al and they belong to spv. Necessary attention was paid for optimum expectation of analytical results. SEM images were used to interpret the microtexture, microstructure shape and size of mineral grains. Hollow tabular crystals of 120x30μm were seen (Fig.-4) with length and breadth ratio 4.

SEM images show that maximum thicknesses of flow-bandings were <5 μm. Several sheets 1 μm of flow one over the other were seen (Fig:-4) Acicular aggregates had length 16 μm and breadth 1.5 μm with ratio over 10. Megastructures are reflected in microstructures. The massive matrix was fine-grained <2 μm. The EDAX analyses at different parts were very similar showing that the lava was a monomineralic rock. Vesicles of varying sizes from 8 to 1 μm were seen. Adjacent to vesicles euhedral minerals occur.

4. GEOCHEMICAL STUDIES

Wet gravimetric analyses are studied (Table1). The difficulties were encountered in separation of R_2O_3. Only total Fe_2O_3 was determined.

Table 1: *Wet gravimetric chemical analyses of perovskite lava samples from different places of Tamil Nadu*

	v1	v2	v4	v5	v6	v7	v8	v11	v12	v13
	FeTiore									
SiO2	15.46	16.09	15.62	14.04	14.42	15.28	14.79	4.35	9.96	7.06
Al2O3	11.25	14.50	7.35	7.18	7.98	13.51	15.90	6.76	4.78	4.63
Fe2O3	42.26	41.43	46.55	51.56	47.37	42.60	41.33	62.64	58.31	65.69
MgO	1.77	1.39	2.57	0.90	1.23	1.12	1.07	0.74	0.00	0.73
CaO	3.93	3.53	6.19	2.94	1.32	4.85	5.02	2.78	3.36	3.77
Na2O	1.18	2.79	0.92	0.99	0.70	0.74	0.64	0.82	0.59	1.02
K2O	1.29	1.54	1.70	1.18	1.10	1.00	1.00	1.05	1.15	1.60
TiO2	19.81	18.57	18.61	20.75	24.39	20.86	20.17	21.57	22.14	15.84
P2O5	0.07	0.05	0.02	0.05	0.02	0.02	0.07	0.23	0.23	0.23
Moi	0.04	0.01	0.60	0.02	1.28	0.07	0.25	0.13	0.12	0.35
`Norm Tr2O3	as		Fe2O3							
	1	2	3	4	5	6	7	8	9	10
ap	0.21	0.20		0.21			0.20	0.58	0.58	0.58
mt	3.14	2.82	4.32	4.89	3.51	2.99	3.02	18.94	5.24	32.97
il	21.95	19.55			40.65	28.13	25.13			
pvs			9.73	1.13				0.44	4.37	7.23
hz	23.69	20.01	13.36	14.89		11.41	15.66	15.31	9.18	4.34
ol			55.96	59.22				54.28	69.12	40.35
bi	39.51	42.32			41.79	36.55	39.45			
ne		10.83	8.90	0.85				10.45	6.26	14.53
pl	7.11	4.27	7.74	18.79	11.61	20.92	16.53		5.24	
qz	4.39				2.44					

Total Fe2O3 includes all Tr2O3 v_1 v_2 karuppur, v_4 kadavur, v_5 Nalluranpatti, v_6 Mylampatti v_7 Sillapatti, v_8 melvenkataporam v_{11-13} Udiyu to Sivamalai

Table 2: *Wet-chemical, infra-red and x-ray analyses*

oxides	wt%	wave No-cm	Transmi	ions	dA	I/Io	elem	6(ions)
SiO2	4.99	3860	90		4.2603	12	Nb	0.494
Al2O3	4.92	3830	90		3.7808	29	Ta	0.030
Fe2O3	2.66	3810	88		3.5857	10	Ti	0.744
FeO	30.48	3730	86	H2O	3.1977	7	Fe3	0.109
MnO	0.46	3690	85	H2 OH	3.0480	17	Si	0.273
MgO	0.74	3433	78	H2O	3.0079	17	Al	0.316
CaO	7.58	2967	75		2.9022	14	Fe	1.396
Na2O	0.79	2930	77		2.8130	100	Mn	0.020
K2O	1.67	2361	58	CO2	2.7217	7	Mg	0.059
TiO2	18.07	2341	72		2.5601	77	Ca	0.445
Tr2O3	27.64	1757	78	H2O	2.3500	14	Na	0.082
	100	1685	83	H2	2.2697	31	K	0.115
Norm	wt%	1399	89	H2O	2.2165	14		2(O)ions
mt	5.40	1048	40	Si	2.0102	17	Ti	0.248
maghe	13.39	873	64	CO2, H2O	1.8799	27	Nb	0.165
cris	15.65	520	18	Ti, H2O	1.8484	10	Ta	0.010
pvs	20.81	448	17	Ti, H2O	1.8275	7	Si	0.091
sc	12.42				1.8071	27	Al	0.105
col	19.27				1.7292	65	Fe3	0.036
hs	7.50				1.7035	12	Fe	0.465
sp	4.19				1.6681	10	Mn	0.007
qz	1.37				1.6380	29	Mg	0.020
					1.5395	12	Ca	0.148
					1.5073	43	Na	0.027
					1.4903	7	K	0.038
					1.4327	29		
					1.4148	22		
					1.3831	22		
					1.3525	19		

At lower magnification the rock was glassy with embryonic crystals with layered microstructure.

The results show that the samples are enriched with SiO_2, Fe_2O_3 (total), TiO_2, Al_2O_3, CaO, MgO, and ZrO_2. The lava is silica under-saturated. Notable amount of Si and Al in pv. It is a spv. The Rittmann's norm [15] indicates presence of perovskite-pvs (pv), ilmenite (il), hercynite (hz) and others. The presence of H_2O is indicated by infra-red spectral analyses (Table-2). Structural formula on the basis of 6 O ions shows almost A and B site of pv are in the ratio of 1:1. On the basis of 3(O) ions for spv A site is extremely enriched over 1 and the B site highly deficiency below 1. The excess ions A site

Table 3: *EDAX analyses without Nb content*

`	1	2	3	4	5
SiO2	47.42	44.80	25.68	24.23	20.31
Al2O3	1.59	2.09	1.35	1.63	1.48
FeO	26.86	27.43	35.11	33.45	37.03
MgO	2.15	2.83	1.83	2.20	1.99
CaO	2.27	3.25	2.68	2.83	3.06
Na2O	0.67	0.00	0.63	1.43	1.05
K2O	1.82	2.69	2.45	2.42	2.13
TiO2	8.48	7.93	18.27	17.61	19.37
P2O5	1.98	2.29	1.86	1.08	1.13
SrO	0.00	0.00	0.00	0.00	0.00
ZrO2	3.13	2.12	3.84	3.96	4.09
HfO2	0.00	0.00	0.79	1.55	1.11
Nb2O5	0.00	0.00	0.00	0.00	0.00
Ta2O5	0.38	0.38	1.13	3.42	2.26
Y2O3	3.25	4.20	4.38	4.20	5.00
	100	100	100	100	100
On the	basis	of	3	oxygen	ions
Si	0.973	0.936	0.590	0.553	0.483
Al	0.039	0.052	0.037	0.044	0.041
Fe	0.461	0.479	0.674	0.639	0.736
Mg	0.066	0.089	0.063	0.075	0.071
Ca	0.048	0.070	0.064	0.067	0.075
Na	0.027	0.000	0.028	0.063	0.049
K	0.048	0.072	0.072	0.070	0.064
Ti	0.140	0.133	0.337	0.323	0.369
P	0.069	0.081	0.072	0.042	0.045
Sr	0.000	0.000	0.000	0.000	0.000
Zr	0.016	0.011	0.021	0.022	0.024
Hf	0.000	0.000	0.051	0.099	0.074
Nb	0.000	0.000	0.000	0.000	0.000
Ta	0.001	0.001	0.004	0.011	0.007
Y	0.024	0.031	0.036	0.034	0.042
	Trace elements				
F	0.00	0.00	0.00	0.42	0.55
Cl	0.00	0.00	0.11	0.06	0.15
S	0.04	0.00	0.11	0.08	0.00
Sc	0.00	0.00	0.23	0.36	0.30
Cu	0.02	0.00	0.04	0.24	0.17
V	0.00	0.08	0.11	0.25	0.00
Co	0.02	0.07	0.26	0.44	0.29
Cr	0.00	0.00	0.12	0.22	0.20
Mn	0.22	0.15	0.44	0.55	0.57
Ni	0.00	0.07	0.08	0.24	0.14
Pb	0.24	0.53	0.74	1.22	0.63
Zn	0.03	0.08	0.10	0.40	0.31
La	0.31	0.10	1.04	1.70	1.31
Ce	0.04	0.00	0.46	1.02	0.59
Nd	0.00	0.00	0.13	0.36	0.17
Eu	0.00	0.00	0.00	0.37	0.16
Yb	0.00	0.00	0.00	0.41	0.00
Dy	1.47	1.58	2.23	2.46	3.02
Lu	0.00	0.00	0.00	0.41	0.00

above 1 are transferred to B site to meet deficiencies in B site to retain electrostatic balances. However, ratios of these elements inTable-3 vary around the structure of pv 1:1 typical structure of pv, spv or ppv.

Table- 4: shows very low contents of Ca and Ti. By entries of Nb, Zr Si and Al to meet the deficiencies Ti, B site is anomalously enriched over A site and therefore, it is termed as spv by Si and Al in B site. Some transition elements REE and gold were also determined at magnified levels. Gold is present an average of 1300 ppm. Dy is present at higher levels. F, Cl and S substitute for oxygen. The distribution of components in variation diagrams for sample 1 (Table-4) is more scattered than sample 2 (Table-5) which is more linear. (Si+Al) vs (Ca+Ti) indicate negative linear trends for samples 1 and 2. Increasing substitution reduces Ca in the A site and Ti in the B site. Sample-2 shows more linear trends. (Na+K+Al+Y) against Ca+Ti shows a positive-linear trend. The distribution of Na+Nb in A site vs Ca in A site show positive linear variation but such variation is more linear in the sample S-2. Similar variation is found Mg vs Fe. The distribution Zr+Hf vs Nb+Ta show more positive linear variation for sample-2. Y against Zr+Hf show better positive linear variation for sample-2. Similarly, the samples S-2, ratio of A site and B site is 1:1 equivalent to pv structure, though B site is slightly higher for abnormal entries of Nb, Zr, Si and Al. The samples show significant enrichments of REE, PGE, Ag, Au, Pb and U metals. The high concentrations of these incompatible elements represent their original inherent concentrations at mantle source [16]. The concentrations of transition-elements, REE, PGE, Ag, Au, Pb and U were determined at magnified levels. The co- variation diagrams show linear trends indicating their genetic relationships.

5. DISCUSSION

Geophysical studies reveal that the lower mantle portion of the Earth is composed of solid phase of pv [17]. It extends up to a depth of 2891 km where CMB exists. It is believed that a major portion of lower mantle is composed of spv. Pv, ilmenite and other pv group of minerals form as high pressure phases in lower mantle. Pv accommodates Nb, Na and K, which entered by substitution of $Ca^{2+} + Ti^{4+} \rightarrow Na^{+} Nb^{5+}$ *and* $2Ti^{4+} \rightarrow Fe^{3+} + Nb^{5+}$. Spv or ppv are unable to stable at Earth's surface [18]. Pv has flexibility to accommodate several other elements in its composition. Pv or spv at near Earth's surface results collapse of its crystal-structure when it transforming into lava stage. The dislocation of deformed spv takes place by creep

Table4: *EDAX analyses with transition elements (sample 1) S-1*

	1	2	3	4	5	6	7	8	9	10	11	12
SiO2	6.07	25.87	22.89	9.32	10.96	9.37	12.20	23.44	18.35	25.41	17.23	15.49
Al2O3	0.61	3.27	2.65	0.78	0.84	0.72	2.70	5.52	3.95	5.03	4.53	2.54
FeO	5.81	10.11	11.86	10.75	10.93	16.25	3.10	6.06	5.61	6.71	5.63	8.81
MgO	0.12	0.39	0.35	0.08	0.03	0.05	0.70	0.97	0.87	0.80	0.98	0.44
CaO	1.96	1.09	1.50	1.50	1.51	2.17	10.39	3.86	3.74	2.78	4.81	3.06
Na2O	0.19	0.63	0.57	0.13	0.06	0.08	1.14	1.58	1.42	1.30	1.60	0.72
K2O	0.23	0.78	0.83	1.10	1.35	0.94	0.64	1.74	1.44	1.00	1.92	1.08
TiO2	0.03	0.21	0.00	0.21	0.26	0.22	0.22	0.48	0.45	0.27	0.48	0.25
P2O5	0.00	0.20	0.23	0.00	0.06	0.10	0.00	0.19	0.20	0.00	0.16	0.10
SrO	2.12	2.58	3.30	3.07	2.96	4.08	2.38	2.52	2.66	1.74	2.49	2.80
ZrO2	8.49	4.70	13.10	9.25	11.26	7.29	8.00	12.28	6.66	10.75	8.16	9.22
HfO2	0.07	0.92	0.56	0.71	0.79	1.34	0.00	1.10	0.63	0.58	0.30	0.64
Nb2O5	64.71	39.87	30.80	48.78	43.94	42.69	50.54	31.54	47.01	34.78	40.05	43.54
Ta2O5	0.15	1.96	1.48	1.92	1.83	2.50	0.34	2.54	1.09	1.08	1.28	1.48
Y2O3	9.44	7.43	9.87	12.39	13.23	12.21	7.66	6.18	5.92	7.76	10.37	9.83
	100	100	100	100	100	100	100	100	100	100	100	100
On the	basis	of	3	oxygen	ions							
Si	0.288	0.800	0.711	0.397	0.442	0.394	0.456	0.692	0.623	0.742	0.578	0.558
Al	0.034	0.119	0.097	0.039	0.040	0.036	0.119	0.192	0.158	0.173	0.179	0.108
Fe	0.230	0.261	0.308	0.383	0.368	0.571	0.097	0.149	0.159	0.164	0.158	0.265
Mg	0.009	0.018	0.016	0.005	0.002	0.003	0.039	0.043	0.044	0.035	0.049	0.024
Ca	0.096	0.035	0.048	0.066	0.063	0.094	0.402	0.118	0.131	0.084	0.167	0.114
Na	0.018	0.038	0.034	0.011	0.004	0.006	0.083	0.091	0.093	0.074	0.104	0.050
K	0.014	0.031	0.033	0.060	0.069	0.050	0.030	0.066	0.062	0.037	0.082	0.050
Ti	0.001	0.005	0.000	0.007	0.008	0.007	0.007	0.011	0.012	0.006	0.013	0.007
P	0.000	0.011	0.012	0.000	0.004	0.007	0.000	0.010	0.012	0.000	0.009	0.006
Sr	0.000	0.004	0.004	0.000	0.002	0.002	0.000	0.003	0.004	0.000	0.003	0.002
Zr	0.196	0.071	0.199	0.192	0.221	0.149	0.146	0.177	0.110	0.153	0.133	0.162
Hf	0.001	0.008	0.005	0.009	0.009	0.016	0.000	0.009	0.006	0.005	0.003	0.007
Nb	2.773	1.115	0.865	1.878	1.602	1.621	1.708	0.841	1.442	0.919	1.214	1.418
Ta	0.001	0.008	0.006	0.011	0.010	0.014	0.002	0.010	0.005	0.004	0.006	0.007
Y	0.159	0.082	0.109	0.187	0.189	0.182	0.102	0.065	0.071	0.080	0.123	0.126
	1	2	3	4	5	6	7	8	9	10	11	12
F	0.06	0.00	0.40	0.15	0.03	0.00	0.95	0.61	0.76	0.70	0.59	0.39
Cl	0.04	0.16	0.20	0.24	0.30	0.31	0.00	0.11	0.09	0.11	0.09	0.15
S	0.02	0.10	0.08	0.14	0.14	0.14	0.03	0.03	0.08	0.04	0.11	0.08
Sc	0.04	0.16	0.22	0.32	0.37	0.51	0.06	0.15	0.10	0.00	0.07	0.18
Ba	0.04	0.00	0.55	0.22	0.34	0.60	0.00	0.37	0.17	0.00	0.37	0.24
V	0.08	0.16	0.13	0.23	0.26	0.38	0.00	0.13	0.08	0.05	0.11	0.15
Co	0.15	0.33	0.30	0.41	0.48	0.43	0.05	0.22	0.06	0.11	0.13	0.24
Ni	0.00	0.16	0.19	0.38	0.31	0.46	0.03	0.20	0.08	0.15	0.19	0.20
Pb	0.39	1.24	1.52	3.28	3.66	1.94	1.05	1.35	1.30	1.57	1.69	1.73
La	0.15	0.74	0.63	0.98	1.17	1.44	0.00	0.45	0.32	0.13	0.28	0.57
Ce	0.07	0.51	0.25	0.61	0.87	0.94	0.00	0.00	0.08	0.00	0.00	0.30
Nd	0.06	0.38	0.38	0.69	0.55	0.82	0.00	0.18	0.09	0.00	0.07	0.29
Eu	0.30	0.43	0.53	0.94	1.06	1.52	0.08	0.42	0.42	0.17	0.43	0.57
Gd	0.26	0.82	0.51	1.22	1.22	1.41	0.00	0.48	0.16	0.13	0.37	0.60
Dy	1.07	1.28	1.27	0.96	2.48	0.70	0.23	0.71	0.57	0.91	0.21	0.94
Lu	0.00	0.70	0.30	0.91	0.32	1.13	0.00	0.46	0.61	0.22	0.26	0.45
Au	0.00	0.28	0.33	0.09	0.10	0.16	0.09	0.00	0.13	0.00	0.24	0.13

mechanism [19]. Sudden development of deep creep during planetary motion at CMB opens vent for escape of plasmatic fluids as microplume. The plasma-plume is developed due to sudden release of pressure at CMB without any loss of heat and temperature of 4000°K. Such plasma-plume ascends so rapidly without any friction along its side walls and loss of its potential energy till it reaches to Earth's surface. The volume expansion is negligible to 0 and loss of heat energy is nil. A Thermodynamic model for existing high pressure (1380 kbars to 1 bar) temperature (4000°K) [20], density of pv or spv is 9.9 g/cm^3. By development of a narrow creep extending to CMB, it is assumed that 1m^3 of material from CMB is ascended to Earth's surface without any expansion or cooling. The material attained by transformation of phases from solid-iquid-gas-plasma. The plasma plume migrated very rapidly up as a double / single walled microplume (Fig-:6) in order to prevent the escape of plasmatic material. On the ideal state of gas laws certain part of solid material within 1m^3 is converted into kinetic energy completely and utilized for rapid upward movement of the plume. The following simple thermodynamic formulae are applied in ideal state of gas laws to construct Table-6:

V–volume; $P=nRT/V$; $V=nRT/P$; n – number of moles;

Table 5: *EDAX analyses with PGE, Ag, Au, Pb and U for S-2*

	1	2	3	4	5	6	7	8	
SiO2	11.94	58.01	6.30	8.56	40.74	11.42	22.21	29.97	
Al2O3	2.73	1.04	1.37	1.05	8.18	2.17	4.53	3.88	
FeO	32.16	10.70	39.08	31.96	7.25	23.14	13.24	13.69	
MgO	2.24	0.55	2.23	2.28	0.73	0.26	2.19	2.53	
CaO	8.45	2.18	6.96	5.39	3.39	15.02	19.65	11.11	
Na2O	0.46	0.57	0.58	1.32	0.93	0.00	2.00	3.77	
K2O	0.55	0.68	0.47	1.07	14.46	1.03	1.68	1.89	
TiO2	9.67	6.17	8.69	15.80	2.81	15.38	6.32	6.99	
P2O5	0.62	0.30	0.47	1.82	0.26	0.00	1.03	0.64	
SrO	0.00	0.00	0.00	0.00	0.00	0.00	0.00	0.00	
ZrO2	5.62	2.92	5.40	5.41	3.36	7.32	4.62	4.58	
HfO2	0.00	0.00	0.00	0.68	0.62	0.27	0.00	0.51	
Nb2O5	16.62	10.43	18.09	15.42	10.66	13.87	15.66	12.50	
Ta2O5	0.80	0.00	0.00	2.17	0.91	1.05	0.00	1.97	
Y2O3	8.14	6.44	10.35	7.08	5.68	9.07	6.87	5.96	
	100	100	100	100	100	100	100	100	
On the	basis	of	3	oxygen	ions				
Si	0.199	0.966	0.105	0.142	0.678	0.190	0.370	0.499	
Al	0.054	0.020	0.027	0.021	0.161	0.043	0.089	0.076	
Fe	0.448	0.149	0.544	0.445	0.101	0.322	0.184	0.191	
Mg	0.056	0.014	0.056	0.057	0.018	0.007	0.055	0.063	
Ca	0.145	0.038	0.120	0.093	0.058	0.259	0.338	0.191	
Na	0.015	0.018	0.019	0.043	0.030	0.000	0.065	0.122	
K	0.012	0.014	0.010	0.023	0.307	0.022	0.036	0.040	
Ti	0.129	0.082	0.116	0.211	0.038	0.205	0.084	0.093	
P	0.018	0.008	0.013	0.051	0.007	0.000	0.029	0.018	
Sr	0.006	0.003	0.005	0.018	0.002	0.000	0.010	0.006	
Zr	0.046	0.024	0.044	0.044	0.027	0.059	0.038	0.037	
Hf	0.000	0.000	0.000	0.003	0.003	0.001	0.000	0.002	
Nb	0.250	0.157	0.272	0.232	0.160	0.209	0.236	0.188	
Ta	0.002	0.000	0.000	0.005	0.002	0.002	0.000	0.004	
Y	0.048	0.038	0.061	0.042	0.034	0.054	0.041	0.035	
Trace elements									
Sc	0.13	0.00	0.05	0.31	0.21	0.33	0.00	0.19	0.15
La	0.73	0.76	0.67	1.53	0.47	1.73	0.00	0.76	0.83
Ce	0.15	0.11	0.18	0.92	0.58	1.00	0.00	0.38	0.42
Nd	0.00	0.00	0.00	0.09	0.19	0.00	0.00	0.19	0.06
Eu	0.69	0.21	1.05	1.03	0.68	1.42	0.23	0.90	0.78
Dy	2.83	1.44	3.63	4.05	0.60	1.86	1.30	2.06	2.22
Tb	0.00	0.00	0.00	0.00	0.53	0.41	0.00	0.49	0.18
Lu	0.00	0.00	0.00	0.00	0.41	0.00	0.00	0.00	0.05
Ru	0.11	0.17	0.16	0.70	0.28	0.00	0.33	0.83	0.32
Rh	0.22	0.30	0.13	0.62	0.40	0.21	0.00	0.75	0.33
Pd	0.22	0.09	0.26	0.56	0.35	0.24	0.00	0.00	0.22
Ag	0.10	0.24	0.11	0.46	0.42	0.24	0.00	0.00	0.20
Os	0.00	0.00	0.17	0.60	0.48	0.67	0.00	1.20	0.39
Ir	0.15	0.30	0.27	0.60	0.59	0.49	0.23	1.52	0.52
Pt	0.00	0.23	0.59	0.51	0.54	0.74	0.00	1.36	0.50
Au	0.00	0.49	0.47	0.60	0.71	1.40	0.55	1.14	0.67
Pb	0.52	0.88	0.70	0.89	1.45	1.08	1.31	1.57	1.05
U	6.85	8.76	7.76	6.68	5.67	9.78	6.49	6.04	7.25

EDAX analyses 8 spots in this lava show relatively higher enrichments of TiO_2 and CaO.

R-gas constant 8.315 J T- Temperature in K;
$dT/dP=T\Delta V/\Delta H$; H-heat content

$E_k = ½ mv^2$; E_k=kinetic energy; m =mass v=velocity

$W=2.303nRT\log_{10} P_1/P_2$ W= work

$W=2.303nRT\log_{10}V_2/V_1$

$K=(2.303*t)*\log_{10}(d_1-d_2)$ d –density

V^g = volume of gas

Using these formulae, step by step evaluations of mass reductions to enhance the potential energies levels

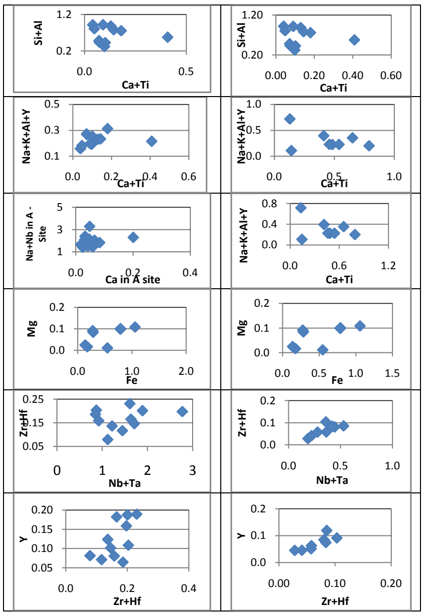

Fig 5: *Variation diagrams of pv, spv or (ppv). Sample 2 in the right side is more linear than sample 1.*

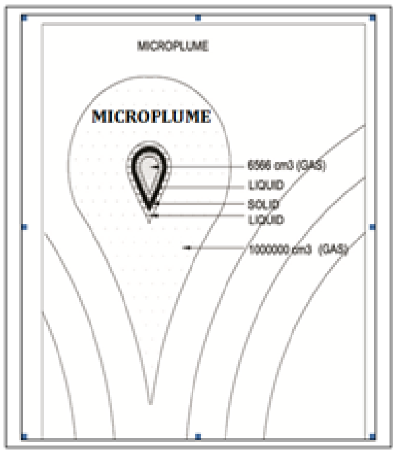

Fig 6: *Model of microplume (plasma-plume) for its rapid ascending from Earth's CMB to land surface.*

were calculated to find out velocity of plasma-plume. Thermodynamic calculations were made by Live-help Hyperphysics [21]. The table shows that the plasma-plume of high density material from deeper part could rise up maximum speed of 288 m/s from CMB to Earth's surface (Fig. 7). On the other hand low density materials from shallower depths could rise up maximum speed of much less than 1cm/s, the latter is subjected by rapid cooling and increasing in its viscosity further lowering speed anomalously. Thus, low viscous high density lava from deep-seated source emplaced on the Earth's surface so rapidly, and it does not have any root or orifice. It is known (Table-6) that molecular speeds were estimated optimum levels of

Table 6: *A thermodynamic model of ideal gas law state for rapid ascending of 1 m^3 from CMB through a sudden creep with pressure reduction from 1380 kbars to 1 bar at 4000°K under friction free and cooling free environment.*

Table 6 Numerical modeling of ascending of a microplume from core-mantle boundary

Depth km	Tempt	p	assumedP	contT	v	const d	const m.wt	const n	const vg
2900	4000	1380	1380000	4000	1m3	9900000	358.79	27593	0.006566
2900	4000	1380	1000	4000		9900000	358.79	27593	0.006566
650	3000	250	1000	4000		9900000	358.79	27593	0.006566
400	2000	15	1000	4000		9900000	358.79	27593	0.006566
100	1000	3.5	1000	4000		9900000	358.79	27593	0.006566
30	600	1	1000	4000		9900000	358.79	27593	0.006566
1	350	0.26	259.9	4000		9900000	358.79	27593	0.006566
0.1	310	0.027	26.89	4000		9900000	358.79	27593	0.006566
0.01	301	0.004	3.589	4000		9900000	358.79	27593	0.006566
0.001	300	0.001	1.259	4000		9900000	358.79	27593	0.006566
0.00001	300	0.001	1	4000		9900000	358.79	27593	0.006566

km2.303*nRT* log10p1/p2 KJ	Excess of free energy KJ	G/U	T Ther flux	Ther fl vg m3	dv Thermal flux	VTherm flux of 1m3-1 1m3 flux	e= 1m3 aureole	e=1m3Aur KJ
917735	917735	1	4000	0.01	0			
12976941	12059206	0.9293	52561	119.07	119.06	118.06	102142401	12059206451
9732706	8814971	0.9057	38421	87.04	87.03	86.03	102463910	8814971088
6488471	5570736	0.8586	24280	55.00	55.00	54.00	103166872	5570735726
3361285	2443550	0.7270	10650	24.13	24.12	23.12	105688198	2443550346
1946541	1028806	0.5285	4484	10.16	10.15	9.15	112418414	1028806218
1243706	325971	0.2621	1421	12.38	12.38	11.38	28651186	325971336
1138801	221066	0.1941	964	81.17	81.17	80.17	2757585	221065672
1365378	447643	0.3279	1951	1231.51	1231.51	1230.51	363787	447642659
1432966	515231	0.3596	2246	4040.71	4040.70	4039.70	127542	515231168
1448818	531083	0.3666	2315	5243.76	5243.76	5242.76	101298	531082739

K=(2.303*t)*log10(d1-d2)

speed m/s	km/hr	m/s+flux	km/hr	V ratio
				1
107	386	185	668	18133
85	307	288	1036	13255
39	142	133	480	8377
38	136	128	460	3674
15	53	50	179	1547
6	22	21	74	1886
3	12	12	41	12362
2	7	6	23	187551
0	1	1	2	615373
0	1	1	2	798591

Table- 6: A model of the buoyant energy of plasma plume moving up to the Earth' surface is shown. At constant temperature of 4000°K, sudden drop of pressure from 1380 kbars how free energies are released up and the residual energies are utilized only for rising up the plasma plume from CMB to land surface step by step. The model illustrates the maximum velocity thrmal flex admixed buoyant 1 m^3 volume of CMB is 288m/s or 1036 km/hr ascending of its own potential energy without any lose of heat by friction

Drop of pressures during ascending plasma plume which is enveloped with an aureole of thermal flux. The table shows that the plume for pv or spv from CMB ascends with maximum speed of 288 m/s. Fluids developed at shallower depths, the speed of the plume drastically reduced much less than1 mm/s (Fig.-7)

6. CONCLUSIONS

The chemical composition and physical properties of Earth's mantle are mysterious. Indirect geophysical experiments show that pv group of minerals occupy major part of lower mantle. It is inferred from meteorites that spv common mineral which occupy the major part of Earth's mantle. Nb bearing with a composition of (Ca, Ce, Y, Na) (Nb, Fe, Ti) O_3 is termed as dysanalyte [22, 23]. The deficiency Ca in A-site in pv is compensated by entry of divalent ions and Ti is replaced by substitution of Zr, Al and Si in B site forming spv. Though Nb and Sr were not determined in some samples (Table-3) collected at Sambavar-vadakarai, they are enriched with Ca, divalent ions, alkalies and REE and in A-site and is higher than 1 and the excessive ions enter into octahedral B site. Though, spv is reported as bridgmanite [24] from meteorites and no natural occurrences on the surface were so far reported. The major part of the mantle is composed of spv [24]. The lava flows of spv appear to be direct evidences for composition of lower mantle. Higher contents of REE, Ag, Au, PGE, Pb and U are due their original inherent enrichment from mantle. Some magma ascends a few cm in thousands of years. Some volcanic effusions might have take-place directly from mantle source very rapidly. It all depends up on its realistic tectonic deformation and mode of emplacement.

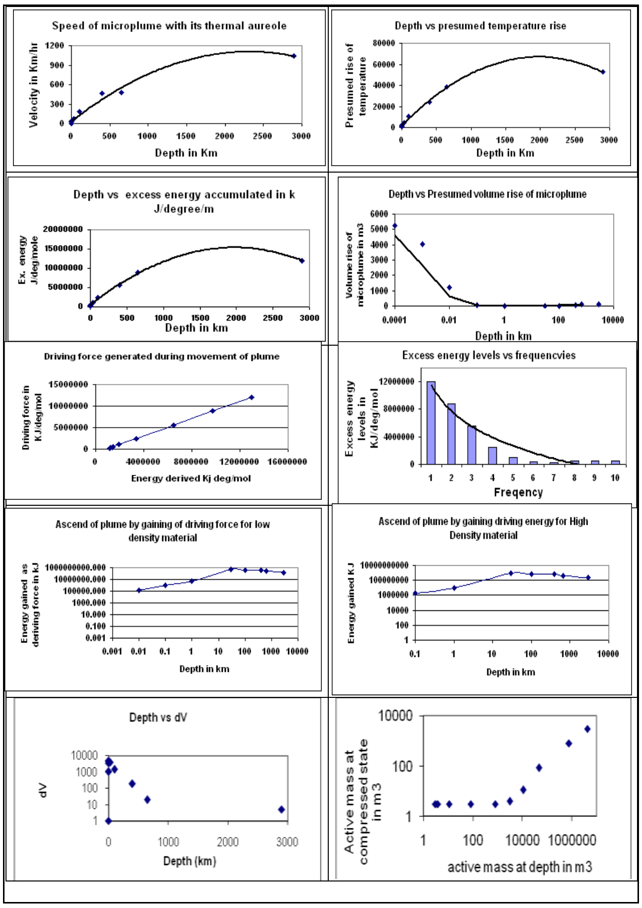

Fig 7: *simplified diagrams showing the residual energy (Table-6) may be utilized for rapid effusion of a low viscous pv or spv lava under ideal gas law state from CMB with maximum speed of 288 m/s to land surface.*

List Item –1 Six Tables

List Item - 2 Seven Figures

List Item –3 Acknowledgement

List Item - 4 Twenty four References, 1-8 p.

ACKNOWLEDGEMENT

The author expresses his sincere thanks to Mr. Vasantha Mohan for his cooperation during field work in Sambavarvadakarai and to T. Ragavaiya, Senior Technician in Metallurgical and Material Science Laboratory, IITM for SEM Images and EDAX analyses.

REFERENCES

[1] D. K. Bailey, *Mantile carbonatite eruptions: Crustal context and implications,* Lithos, vol. 26 [1-2), pp.37-42, December, 1990.

[2] sp.lyellcollection.org/content/30/1/53.refs

[3] D. Francis, and M. Patterson, *Kimberlites and alikites as probes of the continental lithospheric mantle.* Lithos, 109, 72-80. 2009

[4] N.T. Arndt, C.M Lesher,. and S.J. Barnes, *Komatiite,* Cambridge Univ. Press, Cambridge, 488 p 2008.

[5] J. Fontana, *Phoscorite-carbonatite pipe complexex* Platinum Rev. vol.50 (3) p.134 2006.

[6] N. Arndt, C.M. Lesher, G.K. Czamanske. *Mantle-derived magmas and magmatic Ni-Cu- (PGE) deposits.* Economic Geology, 100th Aniversary vol, pp.5-24, 2005.

[7] R. Ramasamy *Geology of the area south-west of Tiruppattur, Tamil Nadu,* Ph.D. Thesis, University of Madras, 226p., 1973.

[8] Max Wilke *Fe in magma-An Over View,* Annals of Geophysics, vol. 48 (4/5), pp. 609-617 Aug-Oct 2005.

[9] R. Ramasamy, Molten rock extrusions, Journal of the Geological Society of India, vol. 55, pp. 337–338, 2000.

[10] National Institute of Geophysical Research Institute, Hyderabad, National Seminar on Plume Tectonics Petrographic observations of lava tube injections and eruptions and spray of volcanic beads in Tamil Nadu and evolution of plume tectonics of Indian Plate Abst. vol, pp,32-33 13-14th June 2000.

[11] K. Hirose, R. Wentzcovitch, D.A. Yuen and T. Lay *Mineralogy of the Deep Mantle – The Post-Perovskite Phase and its Geophysical Significance* In: Gerald Schubert (editor in-chief) Treatise on Geophysics, 2nd edition, Oxford: Elsevier; Vol 2. pp. 85-115 2015.

[12] J. Wookey, S. Stackhouse, J.M/ Kendall, J.P. Brodholt, G.D. Price, *Efficacy of postperovskite as an explanation for lowermost mantle seismic properties*. Nature 438, 1004–1007. 2005.

[13] R, Ramasamy, Sp. Subramanian and R. Sundaravadivelu *Formation of Gas Hydrates at Deep Interior of the Earth and Their Dissipation to Near Surface Horizon,* Journal of Geological Research, vol. 2013, 11p. 2013

[14] R. Ramasamy, *Crystallization, Fractionation and Solidification of Co-Magmatic Alkaline Series Sequentially Emplaced in the Carbonatite Complex of Tiruppattur, Tamil Nadu, India* In Tech Crystallization Science and Technology, Edited by *Marcello Rubens Barsi Andreeta,* Chapter 20 pp.535-564 September 19, 2012.

[15] A. Ritmann Stable Mineral Assemblages of igneous Rocks, Springer-Verlag, Berlin, 264p, 1973.

[16] R. Ramasamy *Noble metal contents in the placer sands of Manavalakurichi, Tamil Nadu,* Internatioal Journal of innovative Sciences and Engineering Technology, vol. 2 (10) October 10p 2016.

[17] https://ww2.kqed.org/science/2014/12/04/earths-most-common-mineral-is-bagged-and-tagged-meet-bridgmanite/

[18] N.L. *Ross, R.M. Hazen High-Pressure Crystal Chemistry of $MgSiO_3$ Perovskite, Physics and Chemistry of Minerals. Vol. 17 pp.228–237, 1990*

[19] P. *Cordier, T. Ungár, L. Zsoldos, G. Tichy Dislocation creep in MgSiO3 perovskite at conditions of the Earth's uppermost lower mantle. Nature. Vol. 428 (6985): pp.837–840, 2004.*

[20] Stacey, J. (1977) Physics of the Earth, 2nd Edn, J. Wiley, New York

[21] C. R. Nave, Ideal gas laws, Thermodynamic calculations, *Live-help HyperPhysics*, Dept. of Physics and Astronomy, Geogia State Univ. 2016.

[22] E. S. Dana *A Text Book of Mineralogy,* Asia Publishing Home, Madras, 851p, 1949.

[23] https://www.mineralienatlas.de/lexikon/index.php/MineralData?lang=en&language=english&mineral=Dysanalyte

[24] O. Tschauner, Chi Ma, J.R. Beckett, C. Prescher. V.B. Prakapenka and G. R. Rossman, *Discovery of Bridgmanite, the most abundant mineral in Earth,* in a shocked meteorite, Science, Vol.346 (6213, pp. 1100-1102, 28 Nov 2014.

AUTHOR'S BIOGRAPHY

Awarded Ph.D. in 1974, PDE in MSU, Russia. Petrologist in Tamilnadu State Dept. of Geology & Mining. Project Consul-tant in DOE & CE IIT